arXiv:1510.01216v1 [math.DS] 5 Oct 2015

Performance analysis and signal design for a stationary signalized ring road

Wen-Long Jin *and Yifeng Yu †

October 6, 2015

Abstract

Existing methods for traffic signal design are either too simplistic to capture realistic traffic characteristics or too complicated to be mathematically tractable. In this study, we attempts to fill the gap by presenting a new method based on the LWR model for performance analysis and signal design in a stationary signalized ring road. We first solve the link transmission model to obtain an equation for the boundary flow in stationary states, which are defined to be time-periodic solutions in both flow-rate and density with a period of the cycle length. We then derive an explicit macroscopic fundamental diagram (MFD), in which the average flow-rate in stationary states is a function of both traffic density and signal settings. Finally we present simple formulas for optimal cycle lengths under five levels of congestion with a start-up lost time. With numerical examples we verify our analytical results and discuss the existence of near-optimal cycle lengths. This study lays the foundation for future studies on performance analysis and signal design for more general urban networks based on the kinematic wave theory.

Keywords: Signalized ring road; LWR model; Link transmission model; Stationary states; Macroscopic fundamental diagram; Cycle length; Start-up lost time.

1 Introduction

Traffic signals have been widely deployed to resolve conflicts among various traffic streams and improve safety of drivers and pedestrians at busy urban intersections. But signalized intersections are also major network bottlenecks, inducing stop-and-go traffic patterns, travel

*Department of Civil and Environmental Engineering, California Institute for Telecommunications and Information Technology, Institute of Transportation Studies, 4000 Anteater Instruction and Research Bldg, University of California, Irvine, CA, USA 92697-3600. Email: wjin@uci.edu. Corresponding author

†Department of Mathematics, University of California, Irvine, CA, USA. Email: yifengy@uci.edu

delays, and vehicle emissions. Many efforts have been devoted to mitigating the congestion effects of isolated and coordinated intersections by optimally designing phase sequences, cycle lengths, green splits, offsets, and other parameters of traffic signals (Papageorgiou et al., 2005).

Most of existing signal design methods employ two types of traffic flow models: aggregate delay and bandwidth formulas or traffic simulation models. In the first type of methods, the cycle length of a signal is selected to minimize vehicles' average delays according to Webster's formula, the allocation of the total effective green time in a cycle to different phases depends on their respective flow-rates, and then offsets at different intersections are determined by optimizing the bandwidth (Miller, 1963; Gartner et al., 1975; Roess et al., 2010). Such an approach is straightforward for designing either pretimed or actuated signals but has serious limitations: first, Webster's formula is derived based on the assumption of random Poisson arrival patterns of vehicles, but in reality arrival patterns are regulated by other signals; second, Webster's formula only applies to under-saturated intersections without accounting for impacts of congested downstream links; third, delay formulas used at the design stage are usually different from those used at the analysis stage (Dion et al., 2004); finally, exact relationships between bandwidths and vehicles' delays are not clear. Therefore, methods based on Webster's and other delay formulas are too simplistic, since they cannot capture traffic waves on a link, interactions among intersections, queue spillback, or other realistic traffic phenomena in a signalized road network. In the second type of methods, various traffic flow models are used to simulate realistic traffic dynamics, and optimal control problems are formulated to find best signal settings simultaneously subject to given demand patterns (Gazis and Potts, 1963; Gazis, 1964; D'ans and Gazis, 1976; Improta and Cantarella, 1984; Papageorgiou, 1995; Park et al., 1999; Chang and Lin, 2000; Chang and Sun, 2004). However, such methods are too detailed to be amenable to mathematical analyses and computationally costly for studying large-scale networks. In summary, existing methods for traffic signal design are either too simplistic to capture realistic traffic characteristics or too complicated to be analytically solvable. We believe that this is major reason for the lack of ''a systematic theory (even) for a one-way arterial'' (Newell, 1989).

The existence of a gap between methods based on delay formulas and those based on traffic simulation has motivated us to develop a new approach for performance analysis and signal design in signalized networks. Our daily experience suggests that traffic patterns in an urban road network are relatively stationary during peak periods; that is, the locations and durations of congestion are stable from day to day. The new approach builds on the assumption of the existence of such stationary states. Furthermore, we attempt to derive the average flow-rate in stationary states as a function of signal settings within the framework of the LWR model (Lighthill and Whitham, 1955; Richards, 1956). In such stationary networks, the average flow-rate can serve as a performance measure and the objective function to find optimal signal settings, since a larger flow-rate at the same density leads to lower average delays and more efficient operations. Therefore, such a method is both physically realistic and mathematically tractable.

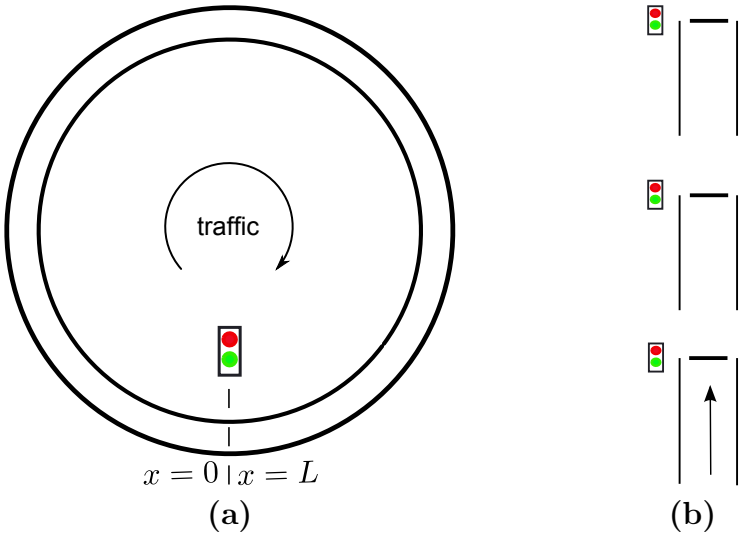

Figure 1: (a) A signalized ring road (b) An infinite street with identical roads

In (Jin and Yu, 2015), it was proved that asymptotic periodic traffic patterns, which can be defined as stationary states, exist in a ring road with a pretimed signal, shown in Figure 1(a). As a first step for developing a unified approach for signal design for general road networks, in this study we start with the signalized ring road, which is the simplest signalized network. The signalized ring road is equivalent to an infinite street without turning movements in Figure 1(b), where all links, traffic conditions, and signal settings are identical. In this sense, the offset between two consecutive signals is 0, and signals follow a simultaneous progression in the northbound direction. In addition, we assume that each cycle has only two phases. Therefore, signal settings remain to be determined include the green split and the cycle length.

In stationary urban road networks, it was postulated that there exits a relation between network-average flow and density in (Godfrey, 1969). Such a relation is called the macroscopic fundamental diagram (MFD) and has been shown to be unique in homogeneous networks, but not in non-homogeneous ones with simulations and observations (Ardekani and Herman, 1987; Mahmassani et al., 1987; Olszewski et al., 1995; Geroliminis and Daganzo, 2008; Buisson and Ladier, 2009; Cassidy et al., 2011; Geroliminis and Boyaci, 2012). In (Daganzo, 2007; Geroliminis et al., 2013), regional demand control strategies were developed based on MFD. As a system-wide characteristic, MFD emerges from network traffic flow patterns, which are determined by network topology, signal and other control measures, and drivers' choices in destinations, modes, departure times, routes, and speeds. Some efforts have been devoted to deriving MFD in simple signalized networks from various traffic flow models. In (Gartner and Wagner, 2004), with cellular automaton simulations for traffic on a ring road, which has multiple identical signals, the relationship between flow-rate, density, and offset was obtained

in relatively stationary states after a long time (2000 seconds), and it was found that offsets can have drastic impacts on the overall throughputs and, therefore, travel times on an arterial road. In (Daganzo and Geroliminis, 2008), a variational method was proposed to calculate approximate MFD in a ring road with multiple signals, but no definitions of stationary states were provided, and impacts of signal settings were not considered. As far as we know, no simple guidelines for signal design were provided in this reference and its follow-up studies, even for a signalized ring road. In (Daganzo et al., 2011), MFD in a double-ring network with turning movements was studied with heuristic double-bin approximations and cellular automaton simulations. In (Jin et al., 2013), steady or stationary states in a signalized double-ring network were defined as asymptotically periodic traffic states within the framework of a network kinematic wave theory, and impacts of signal settings and turning movements on MFD in stationary states were simulated with Cell Transmission Model (CTM) (Daganzo, 1995). However, there has been no theory for the existence of such stationary states in general networks, and no explicit closed-form relation between signal settings and MFD is known, even for simple networks. In this study, we take one step further by deriving the average flow-rate in stationary states as a function of both density and signal settings, which can be used to find optimal signal settings at different congestion levels.

This study is enabled by the link transmission model (LTM) (Yperman et al., 2006; Yperman, 2007), which, together with Newell's simplified kinematic wave model (Newell, 1993), is another formulation of the network kinematic wave theory based on the LWR model. In (Jin, 2015), two continuous formulations of the LTM were derived from the Hopf-Lax formula for the Hamilton-Jacobi equation of the LWR model. [1] For the signalized ring road, we first formulate and solve the LTM for boundary flows (Section 2), then derive an explicit formula for MFD in stationary states and analyze its relationship with signal cycle length (Section 3), and finally find optimal signal settings to maximize the average flow-rate in MFD (Section 4). In Section 5, we conclude the study with future directions.

2 The link transmission model for a signalized ring road

For a ring road with a length of L, as shown in Figure 1(a), the x-axis increases in the traffic direction, and we place a signal at $x = 0$ and $x = L$. We apply the LWR model to describe traffic dynamics in the signalized ring road. Due to the existence of the signal, the problem is much more challenging to solve within the traditional framework of hyperbolic conservation laws. Here we study it with the help of the LTM.

[1] Even though the LWR model was already applied to analyze the formation of queues at a signalized intersection in (Lighthill and Whitham, 1955), no relationships between signal settings and system performance have been established.

2.1 The LWR model and Hamilton-Jacobi equation

The evolution of traffic density $k(x,t)$ on the ring road can be described by the LWR model:

$$\frac{\partial k}{\partial t} + \frac{\partial B(x,t)Q(k)}{\partial x} = 0, \tag{1a}$$

with a periodic boundary condition

$$k(0,t) = k(L,t). \tag{1b}$$

Here we assume a triangular fundamental diagram (Munjal et al., 1971; Haberman, 1977; Newell, 1993),

$$Q(k) = \min\{Vk, (K-k)W\}, \tag{1c}$$

where V is the free-flow speed, $-W$ the shock wave speed in congested traffic, and K the jam density. Thus the critical density is $\bar{K} = \frac{W}{V+W}K$, and the capacity $C = V\bar{K}$.

The effect of the signal is captured by $B(x,t) = 1 - I(x)\cdot(1-\beta(t))$, where $I(x)$ determines the location of the traffic signal: $I(x) = \begin{cases} 1, & x = 0, L \\ 0, & \text{otherwise} \end{cases}$, $\pi \in (0,1)$ is the ratio of effective green time to the cycle length [2], and the traffic light is effective green during $iT + [0, \pi T]$ and effective red during other time intervals:

$$\beta(t) = \begin{cases} 1, & t - iT \in [0, \pi T], \quad i = 0, 1, 2, \cdots \\ 0, & \text{otherwise} \end{cases} \tag{1d}$$

where T is the cycle length.

Following (Newell, 1993), we can obtain the Hamilton-Jacobi equation of the LWR model, (1a), by introducing a new state variable inside the spatial-temporal domain $\Omega = [0, L] \times [0, \infty)$, $A(x,t)$, which is the cumulative flow passing x before t and also known as a Moskowitz function (Moskowitz, 1965). Then $k = -A_x$, $q = A_t$, and the flow conservation equation is automatically satisfied since $A_{xt} = A_{tx}$. Furthermore the fundamental diagram and, therefore, the LWR model for the signalized ring road, (1a), is equivalent to the following Hamilton-Jacobi equation (Evans, 1998):

$$A_t - B(x,t)Q(-A_x) = 0, \tag{2a}$$

with a periodic boundary condition

$$A_t(0,t) = A_t(L,t). \tag{2b}$$

Here the Hamiltonian is both space- and time-dependent, and $-Q(-A_x)$ is convex in A_x for the triangular fundamental diagram. In (Jin and Yu, 2015), the solution of (2a) was proved to be asymptotically periodic, and a relationship between the average density and flow-rate, i.e., MFD, was proved to exist, as the solution of a so-called ‘‘cell problem’’. However, the closed-form equation of MFD was not found.

[2] Here we approximate a cycle, which comprises green, yellow, all red, and red intervals, by an effective green interval and an effective red interval.

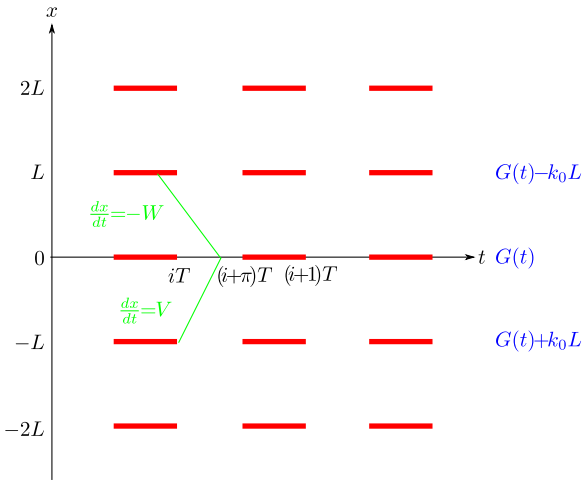

Figure 2: A periodic extension of the spatial-temporal domain Ω

2.2 The link transmission model

As shown in Figure 2, where the red bars denote the effective red light signals, we extend the spatial-temporal domain Ω periodically, since the signalized ring road is equivalent to a street with identical links. We denote the initial condition by $N(x) = A(x, 0)$ and the average density on the ring road by k_0. Then $N(x) = N(x - L) - k_0 L$. We further assume that the initial density is constant at k_0 on all links; i.e., initially $N(x) = -k_0 x$. We denote the boundary flow by $G(t) = A(0, t)$ with $G(0) = 0$ and the corresponding flow-rate by $g(t)$. Then

$$\frac{\mathrm{d}}{\mathrm{d}t} G(t) \quad = \quad g(t). \tag{3}$$

Then from the periodic boundary condition (2b), we have $A(jL, t) = G(t) - jk_0 L$ for $j = 0, \pm 1, \pm 2, \cdots$.

In the following we present the continuous and discrete formulations of LTM, which can be used to solve $G(t)$ both analytically and numerically. Further from $G(t)$, we can solve (2a) to obtain $A(x, t)$ for $x \in (0, L)$ by following Newell's minimization principle (Newell, 1993), Daganzo's variational principle (Daganzo, 2005a,b), the Hopf-Lax formula, optimal control principle, or the viscosity solution method (Evans, 1998). But we are not concerned with traffic dynamics inside the ring road in this study.

In the continuous formulation of LTM (Jin, 2015), we first define the demand, $d(t)$, of the link between $-L$ and 0:

$$d(t) \quad = \quad \begin{cases} \min\left\{k_0 V + H(\lambda(t)), C\right\}, & t \le \frac{L}{V} \\ \min\left\{g(t - \frac{L}{V}) + H(\lambda(t)), C\right\}, & t > \frac{L}{V} \end{cases} \tag{4a}$$

where the link queue size is

$$\lambda(t) \;=\; \begin{cases} k_0 V t - G(t), & t \le \frac{L}{V} \\ G(t - \frac{L}{V}) - G(t) + k_0 L, & t > \frac{L}{V} \end{cases} \tag{4b}$$

Here the indicator function $H(z)$ for $z \ge 0$ is defined as

$$H(z) \;=\; \lim_{\Delta t \to 0^+} \frac{z}{\Delta t} = \begin{cases} 0, & z = 0 \\ +\infty, & z > 0 \end{cases}$$

Then we define the supply, $s(t)$, for the link between 0 and L:

$$s(t) \;=\; \begin{cases} \min\left\{(K - k_0)W + H(\gamma(t)), C\right\}, & t \le \frac{L}{W} \\ \min\left\{g(t - \frac{L}{W}) + H(\gamma(t)), C\right\}, & t > \frac{L}{W} \end{cases} \tag{5a}$$

where the link vacancy size is

$$\gamma(t) \;=\; \begin{cases} (K - k_0)Wt - G(t), & t \le \frac{L}{W} \\ G(t - \frac{L}{W}) - G(t) + (K - k_0)L, & t > \frac{L}{W} \end{cases} \tag{5b}$$

Finally, at the signalized intersection for $x = 0$, we extend the following macroscopic junction model, which was first proposed in CTM (Daganzo, 1995), to calculate the boundary flow-rate:

$$g(t) \;=\; \beta(t) \min\{d(t), s(t)\}. \tag{6}$$

Thus from (3), (4), (5), and (6), we obtain the continuous LTM for the signalized ring road, which is a delay-differential equation with $G(t)$ as the state variable.

The discrete LTM with a time step-size of Δt, where $H(z)\Delta t = z$, can be calculated in the following steps: (i) The discrete link demand is

$$d(t)\Delta t \;=\; \begin{cases} \min\{(t + \Delta t)k_0 V - G(t), C\Delta t\}, & t + \Delta t \le \frac{L}{V} \\ \min\{G(t + \Delta t - \frac{L}{V}) + k_0 L - G(t), C\Delta t\}, & t + \Delta t > \frac{L}{V} \end{cases} \tag{7a}$$

(ii) The discrete link supply is

$$s(t)\Delta t \;=\; \begin{cases} \min\{(t + \Delta t)(K - k_0)W - G(t), C\Delta t\}, & t + \Delta t \le \frac{L}{W} \\ \min\{G(t + \Delta t - \frac{L}{W}) + (K - k_0)L - G(t), C\Delta t\}, & t + \Delta t > \frac{L}{W} \end{cases} \tag{7b}$$

(iii) The discrete boundary flow-rate is

$$g(t)\Delta t \;=\; \beta(t) \min\{d(t)\Delta t, s(t)\Delta t\}. \tag{7c}$$

(iv) The boundary flow can be updated by

$$G(t + \Delta t) \;=\; G(t) + g(t)\Delta t. \tag{7d}$$

From the discrete LTM, we can prove the following theorem, whose proof is given in Appendix A.

Theorem 2.1 *At a large time t, the continuous LTM for a signalized ring road can be solved by the following equation for the boundary flow:*

$$G(t) = \min\{G(t-\frac{L}{V})+k_0L, G(t-\frac{L}{W})+(K-k_0)L, G(iT)+(t-iT)C\}, \quad (8a)$$

for $t-iT \in (0,\pi T]$ during the effective green intervals, and

$$G(t) = G((i+\pi)T), \quad (8b)$$

for $t-iT \in (\pi T, T]$ during the effective red intervals.

Note that, in (8a), three characteristic waves are considered when determining $G(t)$: the first one traveling forward at the free-flow speed, V; the second one traveling backward at the shock wave speed, $-W$; and the third one stationary at $x=0$. In contrast, when solving (2a) inside the ring road with $x \in (0, L)$, only the first two characteristic waves need to be considered. This difference is caused by the existence of the traffic signal at $x=0$.

3 Macroscopic fundamental diagram in stationary states

In (Jin and Yu, 2015), it was shown that time-periodic solutions in both density and flow-rate exist for (2) after a long time, and the period is the signal cycle length, T, with relatively large T, or multiple times of T with relatively small T. In this section, we consider those with a period of T as stationary states in the signalized ring road. We can see that the signalized ring road is in a stationary state if and only if $g(t+T)=g(t)$. In addition, stationary states can also be defined by

$$G(t+T) = G(t) + \bar{g}T, \quad (9)$$

where $\bar{g} \in [0, \pi C]$ is the average flow-rate during a cycle.

In this section, we derive and analyze the macroscopic fundamental diagram (MFD), which is defined as the relationship between the average flow-rate, $\bar{g}$, and density, k_0, as well as signal settings in stationary states.

3.1 Derivation of macroscopic fundamental diagram

We divide the free-flow travel time, $\frac{L}{V}$, by the cycle length, T, to find the modulus, j_1, and the remainder, α_1. That is,

$$\frac{L}{V} = \theta_1 T, \quad \theta_1 = j_1 + \alpha_1, \quad j_1 = \lfloor \frac{L}{VT} \rfloor = 0, 1, \cdots, \quad 0 \le \alpha_1 < 1, \quad (10a)$$

where $\lfloor \cdot \rfloor$ is the floor function. Similarly we divide the shock wave propagation time, $\frac{L}{W}$, by the cycle length, T, to find the modulus, j_2, and the remainder, α_2. That is

$$\frac{L}{W} = \theta_2 T, \quad \theta_2 = j_2 + \alpha_2, \quad j_2 = \lfloor \frac{L}{WT} \rfloor = 0, 1, \cdots, \quad 0 \le \alpha_2 < 1. \quad (10b)$$

Further we define two critical densities, k_1 and k_2, as follows:

$$k_1 \equiv \frac{j_1 + \min\{\frac{\alpha_1}{\pi}, 1\}}{j_1 + \alpha_1}\pi\bar{K}, \tag{11a}$$

$$k_2 \equiv K - \frac{j_2 + \min\{\frac{\alpha_2}{\pi}, 1\}}{j_2 + \alpha_2}\pi\frac{C}{W}. \tag{11b}$$

Then we have the following Lemma.

Lemma 3.1 *k_1 and k_2 satisfy*

$$\pi\bar{K} \le k_1 \le \bar{K} \le k_2 \le K - \pi\frac{C}{W}. \tag{12}$$

In addition, $k_1 = \pi\bar{K}$ if and only if $\alpha_1 = 0$, and $k_1 = \bar{K}$ if and only if $\pi T \ge \frac{L}{V}$; $k_2 = K - \pi\frac{C}{W}$ if and only if $\alpha_2 = 0$, and $k_2 = \bar{K}$ if and only if $\pi T \ge \frac{L}{W}$.

Proof. From the definitions of j_1, α_1, j_2, and α_2 in (10), we can see that $\alpha_1 \le \frac{\alpha_1}{\pi}$ and $\alpha_1 < 1$. Thus $k_1 \ge \pi\bar{K}$, where the equality holds if and only if $\alpha_1 = 0$. In addition, since $\pi < 1$, $k_1 \le \frac{\pi j_1 + \alpha_1}{j_1 + \alpha_1}\bar{K} \le \bar{K}$, where the equality holds if and only if $j_1 = 0$ and $\alpha_1 \le \pi$. That is, $k_1 = \bar{K}$ if and only if $\pi T \ge \frac{L}{V}$. Similarly we can prove $\bar{K} \le k_2 \le K - \pi\frac{C}{W}$: $k_2 = \bar{K}$ if and only if $\pi T \ge \frac{L}{W}$, and $k_2 = K - \pi\frac{C}{W}$ if and only if $\alpha_2 = 0$. Thus (12) is correct. ■

Then LTM during the effective green interval, (8a), leads to

$$\begin{aligned} G(iT + \pi T) = {} & \min\{G((i - j_1)T + (\pi - \alpha_1)T) + k_0 L, G((i - j_2)T + (\pi - \alpha_2)T) + (K - k_0)L, \\ & G(iT) + \pi TC\} = G(iT) + \bar{g}T. \end{aligned}$$

LTM during the red interval, (8b), leads to $G((i+1)T) = G(iT + \pi T)$. Thus in stationary states, from (9) we have $G((i+1)T) = G(iT) + \bar{g}T$ and the following main equation for finding MFD:

$$\begin{aligned} & \min\{G((i - j_1)T + (\pi - \alpha_1)T) + k_0 L, G((i - j_2)T + (\pi - \alpha_2)T) + (K - k_0)L, \\ & G(iT) + \pi TC\} = G(iT) + \bar{g}T. \end{aligned} \tag{13}$$

Since $G(iT) + \bar{g}T \le G(iT) + \pi TC$, $\bar{g} \le \pi C$. Clearly, the average flow-rate πC can only be achieved when the boundary flow-rate is always maximum at capacity during the whole effective green interval; i.e., when $g(t) = C$ for $t - iT \in [0, \pi T]$.

Solving (13), we obtain MFD for the signalized ring road in the following theorem, whose proof is given in Appendix B.

Theorem 3.2 *MFD for the signalized ring road is given by the following piecewise linear function:*

$$\bar{g} = \begin{cases} \frac{k_0}{k_1}\pi C, & 0 \le k_0 < k_1 \\ \pi C, & k_1 \le k_0 \le k_2 \\ \frac{K - k_0}{K - k_2}\pi C, & k_2 < k_0 \le K \end{cases} \tag{14}$$

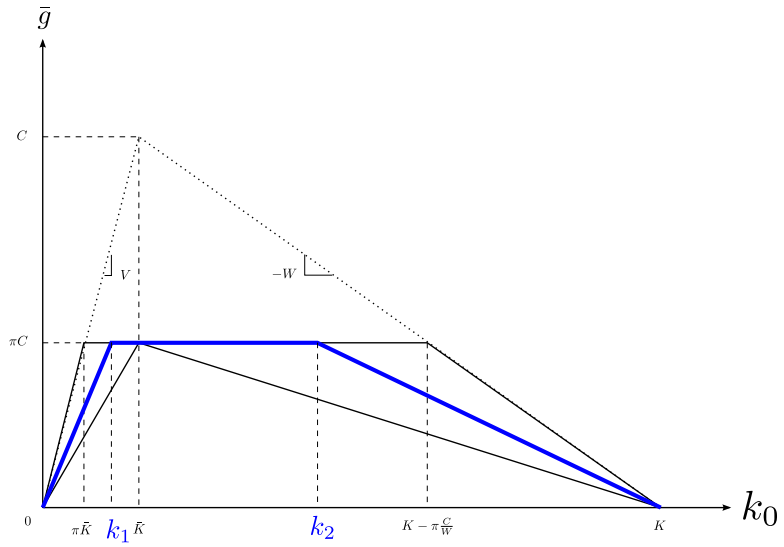

Figure 3: Macroscopic fundamental diagram for a signalized ring road

MFD in (14) is shown in Figure 3, where the dotted lines are for the original triangular fundamental diagram, the thick solid lines for MFD, and the thin solid lines for the boundaries of MFD. The derived MFD has the same shape as those in Figure 2 of (Gartner and Wagner, 2004), which were obtained through simulations. It is also consistent in principle with the piecewise linear MFD in (Daganzo and Geroliminis, 2008), where a numerical method was provided to calculate MFD in a ring road with multiple signals. However, to the best of our knowledge, (14) is the first explicit formula for MFD derived analytically. Such a formula is instrumental for further analysis of system performance and signal design.

Corollary 3.3 *MFD for the signalized ring road can be re-written as*

$$\bar{g} \quad = \quad \min\{\phi_1, \pi C, \phi_2\}, \tag{15}$$

where $\phi_1 = \frac{k_0}{k_1}\pi C$ *and* $\phi_2 = \frac{K-k_0}{K-k_2}\pi C$.

3.2 Properties of MFD

Then from (11) we have the following properties of ϕ_1 and ϕ_2:

1. When $j_1 = 0$ and $0 < \alpha_1 < 1$,

$$\phi_1 \quad = \quad \begin{cases} \pi V k_0, & 0 < \alpha_1 \leq \pi \\ \alpha_1 V k_0, & \pi < \alpha_1 < 1 \end{cases} \tag{16a}$$

When $j_1 \geq 1$ and $0 \leq \alpha_1 < 1$,

$$\phi_1 = \begin{cases} \frac{j_1+\alpha_1}{\pi j_1+\alpha_1}\pi V k_0, & 0 \leq \alpha_1 \leq \pi \\ \frac{j_1+\alpha_1}{j_1+1} V k_0, & \pi < \alpha_1 < 1 \end{cases} \tag{16b}$$

Thus ϕ_1 is continuous in θ_1; ϕ_1 retains the global minimum $\pi V k_0$ when $0 < \theta_1 = \alpha_1 \leq \pi$, reaches global maximum $V k_0$ when $\theta_1 = j_1$, and reaches local minima $\frac{j_1+\pi}{j_1+1} V k_0$ when $\theta_1 = j_1 + \pi$.

2. When $j_2 = 0$ and $0 < \alpha_2 < 1$,

$$\phi_2 = \begin{cases} \pi(K-k_0)W, & 0 < \alpha_2 \leq \pi \\ \alpha_2(K-k_0)W, & \pi < \alpha_2 < 1 \end{cases} \tag{17a}$$

When $j_2 \geq 1$ and $0 \leq \alpha_2 < 1$,

$$\phi_2 = \begin{cases} \frac{j_2+\alpha_2}{\pi j_2+\alpha_2}\pi(K-k_0)W, & 0 \leq \alpha_2 \leq \pi \\ \frac{j_2+\alpha_2}{j_2+1}(K-k_0)W, & \pi < \alpha_2 < 1 \end{cases} \tag{17b}$$

Thus ϕ_2 is continuous in θ_2; ϕ_2 retains the global minimum $\pi(K-k_0)W$ when $0 < \theta_2 = \alpha_2 \leq \pi$, reaches global maximum $(K-k_0)W$ when $\theta_2 = j_2$, and reaches local minima $\frac{j_2+\pi}{j_2+1}(K-k_0)W$ when $\theta_2 = j_2 + \pi_2$.

Since $\theta_1 = \frac{L}{V}\frac{1}{T}$, and $\theta_2 = \frac{L}{W}\frac{1}{T}$, we can have the following $\phi_1 \sim T$ and $\phi_2 \sim T$ relations.

Lemma 3.4 *ϕ_1 and ϕ_2 are functions of T, as shown in Figure 4:*

1. *ϕ_1 is continuous in T; ϕ_1 retains the global minimum $\pi V k_0$ when $T \geq \frac{1}{\pi}\frac{L}{V}$, reaches global maximum $V k_0$ when $T = \frac{1}{j_1}\frac{L}{V}$, and reaches local minima $\frac{j_1+\pi}{j_1+1} V k_0$ when $T = \frac{1}{j_1+\pi}\frac{L}{V}$. In particular, when $\frac{L}{V} \leq T \leq \frac{1}{\pi}\frac{L}{V}$, the $\phi_1 \sim T$ relation for the last decreasing branch is given by:*

$$\phi_1 = \frac{k_0 L}{T}. \tag{18}$$

2. *ϕ_2 is continuous in T; ϕ_2 retains the global minimum $\pi(K-k_0)W$ when $T \geq \frac{1}{\pi}\frac{L}{W}$, reaches global maximum $(K-k_0)W$ when $T = \frac{1}{j_2}\frac{L}{W}$, and reaches local minima $\frac{j_2+\pi}{j_2+1}(K-k_0)W$ when $T = \frac{1}{j_2+\pi}\frac{L}{W}$. In particular, when $\frac{L}{W} \leq T \leq \frac{1}{\pi}\frac{L}{W}$, the $\phi_2 \sim T$ relation for the last decreasing branch is given by:*

$$\phi_2 = \frac{(K-k_0)L}{T}. \tag{19}$$

From (15), we can see that the average flow-rate decreases in k_1 and increases in k_2. In particular, we have the following lemma.

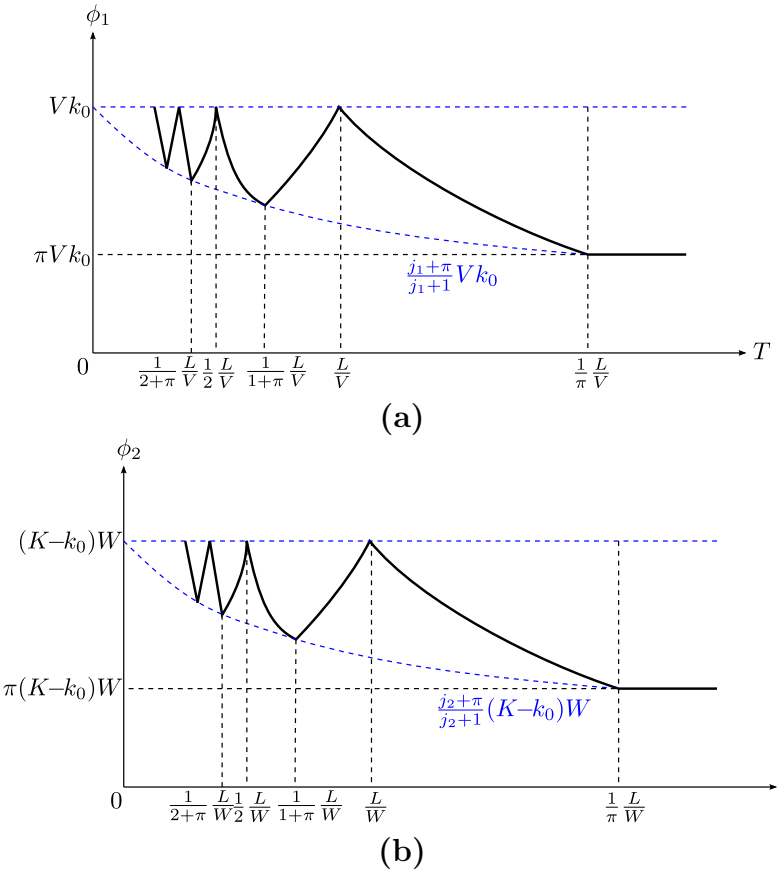

Figure 4: (a) $\phi_1 \sim T$ and (b) $\phi_2 \sim T$ relations

Lemma 3.5 *In five regions for k_0, the average flow-rate varies with $k_1 \in [\pi\bar{K}, \bar{K}]$ and $k_2 \in [\bar{K}, K - \pi\frac{C}{W}]$ as follows:*

1. *When $k_0 \in [0, \pi\bar{K})$; i.e., traffic is very sparse, $\bar{g} = \phi_1$ for $k_1 \in [\pi\bar{K}, \bar{K}]$, which decreases in k_1 and is independent of k_2. In this case, the global maximum flow-rate is Vk_0 when $T = \frac{1}{j_1}\frac{L}{V}$, and the global minimum flow-rate is πVk_0 when $T \geq \frac{1}{\pi}\frac{L}{V}$.*

2. *When $k_0 \in [\pi\bar{K}, \bar{K})$; i.e., traffic is sparse, $\bar{g} = \min\{\phi_1, \pi C\}$, which is first constant for $k_1 \in [\pi\bar{K}, k_0]$ and then decreasing for $k_1 \in (k_0, \bar{K}]$, and independent of k_2. In this case, the global maximum flow-rate is πC, and the global minimum flow-rate is πVk_0 when $T \geq \frac{1}{\pi}\frac{L}{V}$.*

3. *When $k_0 = \bar{K}$; i.e., traffic is critical, $\bar{g} = \pi C$, which is constant for any k_1 and k_2.*

4. *When $k_0 \in (\bar{K}, K - \pi\frac{C}{W}]$; i.e., traffic is dense, $\bar{g} = \min\{\phi_2, \pi C\}$, which is first increasing for $k_2 \in [\bar{K}, k_0)$ and then constant for $k_2 \in [k_0, K - \pi\frac{C}{W}]$, and independent of k_1. In this case, the global maximum flow-rate is πC, and the global minimum flow-rate is $\pi(K - k_0)W$ when $T \geq \frac{1}{\pi}\frac{L}{W}$.*

5. *When $k_0 \in (K - \pi\frac{C}{W}, K]$; i.e., traffic is very dense, $\bar{g} = \phi_2$ for $k_2 \in [\bar{K}, K - \pi\frac{C}{W}]$, which increases in k_2 and is independent of k_1. In this case, the global maximum flow-rate is $(K - k_0)W$ when $T = \frac{1}{j_2}\frac{L}{W}$, and the global minimum flow-rate is $\pi(K - k_0)W$ when $T \geq \frac{1}{\pi}\frac{L}{W}$.*

From Lemmas 3.4 and 3.5, we can then determine $\bar{g}$ for any cycle length, T, at a given density, k_0.

4 Optimal signal settings

In this section, we apply the analytical MFD formula, (14), to find optimal signal settings to minimize the total travel time in stationary states, which is the time for all vehicles to traverse the whole road link and equals $\int_0^T A(0,t) - A(L,t)dt = \frac{(k_0 L)^2}{\bar{g}}$, since $A(0,t) = G(t)$, $A(L,t) = G(t) - k_0 L$, the period equals $T = \frac{k_0 L}{\bar{g}}$. Here we obtain a delay formula for the stationary ring road, $\frac{(k_0 L)^2}{\min\{\phi_1, \pi C, \phi_2\}}$, which is a function both density and signal settings. At a given density k_0, therefore, the objective is equivalent to maximize the average flow-rate $\bar{g}$ and from (15) we have:

$$\max \bar{g} = \max \min\{\phi_1, \pi C, \phi_2\}. \tag{20}$$

If π is constant and independent of T, we can see from Lemmas 3.4 and 3.5 that there are an infinite number of solutions of T for (20):

1. when $k_0 < \bar{K}$, $\bar{g}$ reaches the global maximum, $\bar{g}^* = \min\{Vk_0, \pi C\}$, when $T^* = \frac{1}{j_1}\frac{L}{V}$ for any $j_1 = 1, 2, \cdots$;

2. when $k_0 = \bar{K}$, any T yield the same maximum flow-rate, $\bar{g}^* = \pi C$;

3. when $k_0 > \bar{K}$, $\bar{g}$ reaches the global maximum, $\bar{g}^* = \min\{(K - k_0)W, \pi C\}$, when $T^* = \frac{1}{j_2}\frac{L}{W}$ for any $j_2 = 1, 2, \cdots$.

Since $\bar{g} \geq \frac{j_1+\pi}{j_1+1}Vk_0$ for $k_0 < \bar{K}$ and $\bar{g} \geq \frac{j_2+\pi}{j_2+1}(K - k_0)W$ for $k_0 > \bar{K}$, $\bar{g} \to \bar{g}^*$ when $T \to 0$. That is, we can set the cycle length to be very small to achieve the best performance. In other words, it is best to install stop signs, which correspond to very small cycle lengths.

In reality, however, due to limited reaction times and bounded acceleration rates of drivers and vehicles, there exists a start-up lost time, and π depends on T.

4.1 Analytical solutions with a start-up lost time

We denote the start-up lost time in each phase by δ. Then the total effective green time for a cycle with two phases is only $T - 2\delta$. We assume that the effective green ratio is π_0, which allocates the total effective green time $T - 2\delta$ to the ring road. Then the effective green time is $\pi T = (T - 2\delta)\pi_0$. Therefore we have the following time-dependent ratio

$$\pi \;=\; (1 - \frac{2\delta}{T})\pi_0. \tag{21}$$

Therefore the average flow-rate $\bar{g}$ is bounded by

$$\pi C \;=\; (1 - \frac{2\delta}{T})\pi_0 C, \tag{22}$$

which equals 0 when $T = 2\delta$ and increases in T.

Thus the objective function for the optimal control problem becomes

$$\max \bar{g} = \max \min\{\phi_1, (1 - \frac{2\delta}{T})\pi_0 C, \phi_2\}, \tag{23}$$

where $T \geq 2\delta$. From Lemmas 3.4 and 3.5, we can see that in general ϕ_1 and ϕ_2 decreases in T when π is constant. Therefore it is possible to find a best cycle length to maximize the average flow-rate.

The average flow-rate, $\bar{g} = \min\{\phi_1, (1 - \frac{2\delta}{T})\pi_0 C, \phi_2\}$, is a function of L, K, V, W, π_0, δ, T, and k_0. Among these parameters, L is determined by the road design and layout, K by vehicle lengths and drivers' safety margins, V by speed limit, W by drivers' following aggressiveness, π_0 by effective green time allocation, δ by drivers' reaction times and vehicles' acceleration rates when a light turns green, T by signal lengths, and k_0 by demand levels. In this study, we only consider the impacts of the three signal related parameters, π_0, δ, and T.

First, (14) can be written as

$$\bar{g} \;=\; \begin{cases} \frac{k_0}{j_1+\min\{\frac{\alpha_1}{\pi},1\}}\frac{L}{T}, & 0 \le k_0 < k_1 \\ \pi C, & k_1 \le k_0 \le k_2 \\ \frac{K-k_0}{j_2+\min\{\frac{\alpha_2}{\pi},1\}}\frac{L}{T}, & k_2 < k_0 \le K \end{cases} \tag{24}$$

from which we can see that a larger π leads to higher $\bar{g}$. Further from (21) we can see that π increases in π_0 and decreases in δ. Thus, without changing other parameters, if we reduce the lost time δ and increase the effective green ratio π_0, we can increase the average flow-rate. The lost time, δ, could be reduced by introducing autonomous or connected vehicles, which can have faster responses due to advanced sensors or communications between vehicles and traffic lights. However, the choice of π_0 has to be determined by the demand levels of other competing movements and is assumed to be constant. Thus here we assume that both δ and π_0 are fixed and aim to find an optimal cycle length.

When $\frac{L}{V}$ and $\frac{L}{W}$ are much larger than 2δ (e.g., 10 times), $\pi \approx \pi_0$. Thus we assume that π equals π_0 in ϕ_1 and ϕ_2. But note that the start-up lost time still impacts the average flow-rate in the MFD, as π still depends on T in (22). Then solutions to the optimization problem, (23), are given by the following theorem.

Theorem 4.1 *The optimal cycle lengths at different traffic densities are in the following:*

1. *When traffic is very sparse with $k_0 \in [0, \pi_0\bar{K})$, the maximum $\bar{g}^* \approx Vk_0$, for which there exist multiple optimal cycle lengths:*

$$T^* = \frac{1}{j_1}\frac{L}{V}, \tag{25a}$$

   for $j_1 = 1, 2, \cdots$ and $Vk_0 \le (1 - \frac{2\delta}{T^*})\pi_0 C$.

2. *When traffic is sparse with $k_0 \in [\pi_0\bar{K}, \bar{K})$, the maximum $\bar{g}$ is determined by the intersection between πC and the last decreasing branch of ϕ_1 described by (18):*

$$\bar{g}^* \approx \max_{T\in[\frac{L}{V}, \frac{1}{\pi_0}\frac{L}{V}]} \min\{\frac{k_0 L}{T}, (1 - \frac{2\delta}{T})\pi_0 C\},$$

   for which there exists a unique optimal cycle length

$$T^* \;=\; \frac{k_0 L}{\pi_0 C} + 2\delta. \tag{25b}$$

3. *When traffic is critical with $k_0 = \bar{K}$, the maximum $\bar{g}$ is determined by πC:*

$$\bar{g}^* \approx \max_T \min\{(1 - \frac{2\delta}{T})\pi_0 C\},$$

   fow which there exists a unique optimal cycle length

$$T^* \;=\; \infty. \tag{25c}$$

4. *When traffic is dense with $k_0 \in (\bar{K}, K - \pi\frac{C}{W}]$, the maximum $\bar{g}$ is determined by the intersection between πC and the last decreasing branch of ϕ_2 described by (19):*

$$\bar{g}^* \approx \max_{T\in[\frac{L}{W},\frac{1}{\pi_0}\frac{L}{W}]} \min\{\frac{(K-k_0)L}{T}, (1-\frac{2\delta}{T})\pi_0 C\},$$

for which there also exists a unique optimal cycle length

$$T^* \;=\; \frac{(K-k_0)L}{\pi_0 C} + 2\delta. \tag{25d}$$

5. *When traffic is very dense with $k_0 \in (K - \pi\frac{C}{W}, K]$, the maximum $\bar{g}^* \approx (K-k_0)W$, for which there exist multiple optimal cycle lengths:*

$$T^* = \frac{1}{j_2}\frac{L}{W}, \tag{25e}$$

for $j_2 = 1, 2, \cdots$ and $(K-k_0)W \le (1-\frac{2\delta}{T^*})\pi_0 C$.

Proof. The proof is straightforward, based on Lemmas 3.4 and 3.5 as well as (21), and thus omitted. ■

If we denote the congestion level by

$$\chi \;=\; \frac{\min\{Vk_0, C\}}{\min\{C, (K-k_0)W\}}, \tag{26}$$

which is the ratio of stationary demand over supply, then we have the following corollary from Theorem 4.1.

Corollary 4.2 *The optimal cycle lengths at different congestion levels are in the following:*

1. *When traffic is very sparse with $\chi \in [0, \pi_0)$, the multiple optimal cycle lengths are*

$$T^* = \frac{1}{j_1}\frac{L}{V},$$

for $j_1 = 1, 2, \cdots$ and $Vk_0 \le (1-\frac{2\delta}{T^*})\pi_0 C$.

2. *When traffic is sparse with $\chi \in [\pi_0, 1)$, there exists a unique optimal cycle length*

$$T^* \;=\; \chi\frac{L}{\pi_0 V} + 2\delta, \tag{27a}$$

3. *When traffic is critical with $\chi = 1$, there exists a unique optimal cycle length*

$$T^* \;=\; \infty.$$

4. When traffic is dense with $\chi \in (1, \frac{1}{\pi_0}]$, there exists a unique optimal cycle length

$$T^* = \frac{1}{\chi}\frac{L}{\pi_0 W} + 2\delta. \tag{27b}$$

5. When traffic is very dense with $\chi \in (\frac{1}{\pi_0}, \infty)$, there exist multiple optimal cycle lengths:

$$T^* = \frac{1}{j_2}\frac{L}{W},$$

for $j_2 = 1, 2, \cdots$ and $(K - k_0)W \le (1 - \frac{2\delta}{T^*})\pi_0 C$.

When $\chi < 1$, traditionally Webster's formula has been used to find the optimal cycle length (Roess et al., 2010): even though (27a) is substantially different from Webster's optimal cycle length formula, it is consistent in principle with the latter, as it increases in both the congestion level and the lost time. But here we also obtain a simple formula (27b) when $\chi > 1$, and the optimal cycle length still increases in the lost time but decreases in the congestion level. In addition, the new formulas are derived from the LWR model and, therefore, more realistic.

4.2 Numerical examples

For a signalized ring road we choose the following parameters: $L = 1200$ m, $V = 20$ m/s, $W = 5$ m/s, $K = 1/7$ veh/m, $\delta = 3$ s, and $\pi_0 = \frac{1}{2}$. Then $\pi_0\bar{K} = \frac{1}{2}\bar{K}$, $K - \pi_0\frac{C}{W} = 3\bar{K}$, and $K = 5\bar{K}$.

In Figure 5 we show the average flow-rates, calculated from (14), for different cycle lengths and densities. As shown in Figure 5(a), when traffic is very sparse ($k_0 < \pi_0\bar{K}$), there exist multiple optimal cycle lengths, including $\frac{L}{V}$ and $\frac{1}{2}\frac{L}{V}$. As shown in Figure 5(b), when traffic is sparse ($k_0 \in [\pi_0\bar{K}, \bar{K})$), there exists a unique optimal cycle length greater than $\frac{L}{V}$ but smaller than $2\frac{L}{V}$: $T^* = \frac{k_0 L}{\pi_0 C} + 2\delta$; in this case, $T = \frac{L}{V}$ still leads to near-optimal performance, but $T = 2\frac{L}{V}$ is not acceptable, since the average flow-rate reaches the global minimum when $T = \frac{1}{\pi_0}\frac{L}{V} + 2\delta$. As shown in Figure 5(c), when traffic is dense ($k_0 \in (\bar{K}, K - \pi_0\frac{C}{W}]$), there exists a unique optimal cycle length greater than $\frac{L}{W}$ but smaller than $2\frac{L}{W}$: $T^* = \frac{(K-k_0)L}{\pi_0 C} + 2\delta$; in this case, $T = \frac{L}{W}$ and even $T = \frac{1}{2}\frac{L}{W}$ would lead to near-optimal performance. From Figure 5(d), we can see that, when traffic is very dense ($k_0 > K - \pi_0\frac{C}{W}$), there can exist multiple optimal cycle lengths; in this case, $T = \frac{1}{2}\frac{L}{W}$ would lead to near-optimal performance, and $T = \frac{1}{4}\frac{L}{W}$ is also acceptable for very congested networks. These observations are consistent with the predictions in Theorem 4.1. In addition, from all the figures we can see that the maximum average flow-rate is unimodal in k_0; i.e., $\max \bar{g}$ increases in k_0 until $\bar{K}$ and then decreases.

From Figure 5(b) and Figure 5(c), we can see that πC slowly increases in T when $T \ge \frac{L}{V}$. Therefore, we can choose a cycle length of $\frac{L}{V} = 60$ s for sparse traffic and $\frac{1}{2}\frac{L}{W} = 120$ s

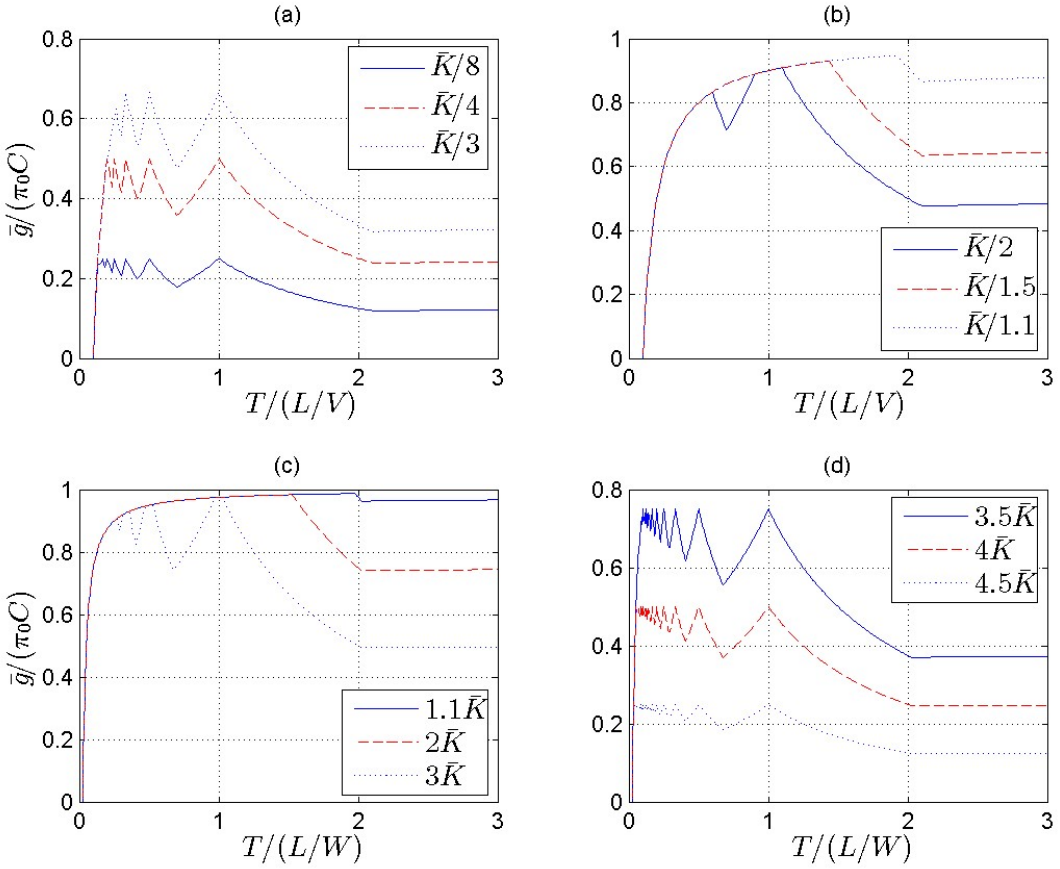

Figure 5: Average flow-rates vs cycle lengths for different densities with a start-up lost time: (a) very sparse traffic with $k_0 \in (0, \pi_0 \bar{K})$; (b) sparse traffic with $k_0 \in [\pi_0 \bar{K}, \bar{K})$; (c) dense traffic with $k_0 \in (\bar{K}, K - \pi_0 \frac{C}{W}]$; (d) very dense traffic with $k_0 \in (K - \pi_0 \frac{C}{W}, K)$

for dense traffic. Such cycle lengths can lead to near-optimal performance. For examples, when $k_0 = \bar{K}/1.5$, $\max \bar{g} = 0.93\pi_0 C$, and $\bar{g} = 0.9\pi_0 C$, which is about 3% smaller, when $T = \frac{L}{V}$; when $k_0 = 2\bar{K}$, $\max \bar{g} = 0.98\pi_0 C$, and $\bar{g} = 0.95\pi_0 C$, which is also about 3% smaller, when $T = \frac{1}{2}\frac{L}{W}$. However, when $k_0 = \bar{K}/1.5$, we cannot choose $T = 2\frac{L}{V} = 120$ s or larger, which leads to an average flow-rate of $0.67\pi_0 C$, about 28% smaller than the maximum value; similarly, when $k_0 = 2\bar{K}$, we cannot choose $T = 2\frac{L}{W} = 480$ s. Furthermore, when traffic is extremely sparse with $k_0 \leq \frac{\bar{K}}{4}$ shown in Figure 5(a) or when traffic is very dense with $k_0 > K - \pi_0 \frac{C}{W}$ shown in Figure 5(d), stop signs, which can be considered as signals with very short cycle lengths, will be as effective as signals.

5 Conclusion

In this paper, we solved the link transmission model to obtain an equation for the boundary flow on a ring road with a pretimed signal. We then defined stationary states as periodic solutions with the cycle length as a period and derived the macroscopic fundamental diagram, from which we can calculate the average flow-rate from density and cycle length. After analyzing the impacts of the cycle length on the average flow-rate, we analytically derived optimal cycle lengths to maximize the average flow-rate subject to realistic start-up lost times due to drivers' reaction and acceleration behaviors. With numerical simulations, we verified the optimal solutions and suggested near-optimal cycle lengths under different congestion levels.

For the simplest signalized network, this study successfully fills the gap between methods based on delay formulas and those based on traffic simulation by presenting a new method that is both physically realistic and mathematically tractable. There are three particular contributions in this study. First, we obtained a simple link transmission model for the boundary flows on a signalized ring road, (8), which forms the foundation for solving and analyzing stationary states. Second, we derived an explicit macroscopic fundamental diagram, (14), in which the average flow-rate is a function of both traffic density and signal settings. Third, we presented formulas for optimal cycle lengths, (27), under five levels of congestion with a start-up lost time.

Even though it has been verified that the analytical optimal cycle length is quite accurate for large free-flow travel and shock wave propagation times, it is still important to check the results for really short links, where these times are small compared with the lost time. In the numerical solutions in Section 4.2, we found that some near-optimal cycle lengths can be used to avoid really long cycle lengths when the road is congested. But we will be interested in rigorously discussing such an optimization problem.

This study for the simplest signalized network is a starting point for developing a unified framework for analyzing and designing signals in other networks, including streets with heterogeneous links and intersections, where cycle lengths, effective green ratios, offsets, and speed limits may be optimized simultaneously. In addition, in this study, we analyze the

performance of an open-loop control system and derive optimal cycle lengths for pretimed signals on a stationary signalized ring road, in which the plant is the whole traffic system, and the actuation is the signal. In the future, we will be interested in introducing feedback control mechanism to develop optimal signal settings under dynamic traffic conditions with random disturbances in general road networks.

Appendix A. Proof of Theorem 2.1

Proof. At a large time $t > \frac{L}{W}$, the discrete LTM, (7), can be written as

$$\begin{aligned} G(t+\Delta t) &= G(t) + \beta(t)\min\{C\Delta t, \\ &\quad G(t+\Delta t-\frac{L}{V}) + k_0 L - G(t), G(t+\Delta t-\frac{L}{W}) + (K-k_0)L - G(t)\}. \end{aligned}$$

Then (8b) is obvious for $t - iT \in (\pi T, T]$. In the following we prove that (8a) is true for $t - iT \in (0, \pi T]$.

For $t - iT \in (0, \pi T]$ during the green intervals, $\beta(t) = 1$, and

$$G(t+\Delta t) = \min\{G(t+\Delta t-\frac{L}{V}) + k_0 L, G(t+\Delta t-\frac{L}{W}) + (K-k_0)L, C\Delta t + G(t)\}.$$

We denote $\Delta t = \frac{\pi T}{n}$. For $j = 1$, we have

$$G(iT+\Delta t) = \min\{G(iT+\Delta t-\frac{L}{V}) + k_0 L, G(iT+\Delta t-\frac{L}{W}) + (K-k_0)L, C\Delta t + G(iT)\}.$$

We assume for any $1 \le j < n$,

$$G(iT+j\Delta t) = \min\{G(iT+j\Delta t-\frac{L}{V}) + k_0 L, G(iT+j\Delta t-\frac{L}{W}) + (K-k_0)L, Cj\Delta t + G(iT)\}.$$

Then for $j+1$, we have

$$\begin{aligned} G(iT+(j+1)\Delta t) &= \min\{G(iT+(j+1)\Delta t-\frac{L}{V}) + k_0 L, G(iT+(j+1)\Delta t-\frac{L}{W}) + (K-k_0)L, \\ &\quad C\Delta t + G(iT+j\Delta t)\}, \\ &= \min\{G(iT+(j+1)\Delta t-\frac{L}{V}) + k_0 L, G(iT+(j+1)\Delta t-\frac{L}{W}) + (K-k_0)L, \\ &\quad C\Delta t + G(iT+j\Delta t-\frac{L}{V}) + k_0 L, C\Delta t + G(iT+j\Delta t-\frac{L}{W}) + (K-k_0)L, \\ &\quad C\Delta t + Cj\Delta t + G(iT)\}. \end{aligned}$$

Since $G(iT+(j+1)\Delta t-\frac{L}{V}) \le C\Delta t + G(iT+j\Delta t-\frac{L}{V})$ and $G(iT+(j+1)\Delta t-\frac{L}{W}) \le C\Delta t + G(iT+j\Delta t-\frac{L}{W})$, we have

$$\begin{aligned} G(iT+(j+1)\Delta t) &= \min\{G(iT+(j+1)\Delta t-\frac{L}{V}) + k_0 L, G(iT+(j+1)\Delta t-\frac{L}{W}) + (K-k_0)L, \\ &\quad C(j+1)\Delta t + G(iT)\}. \end{aligned}$$

Thus from the method of induction, we have for $j = 1, \cdots, n$

$$G(iT + j\Delta t) \;=\; \min\{G(iT + j\Delta t - \frac{L}{V}) + k_0 L, G(iT + j\Delta t - \frac{L}{W}) + (K - k_0)L, Cj\Delta t + G(iT)\}.$$

If we denote $t = iT + j\Delta t$ $(1 \le j \le n)$, then we obtain (8a). ■

Appendix B. Proof of Theorem 3.2

Proof. We derive (14) in the following three cases.

1. From (13), we can see that $\bar{g} = \pi C$ if and only if

$$\begin{aligned} G((i - j_1)T + (\pi - \alpha_1)T) + k_0 L &\ge G(iT) + \pi TC, \\ G((i - j_2)T + (\pi - \alpha_2)T) + (K - k_0)L &\ge G(iT) + \pi TC. \end{aligned}$$

   For the first equation, we have the following two scenarios:

   (a) If $\pi \le \alpha_1$, then $i - j_1 - 1 + \pi < i - j_1 + \pi - \alpha_1 \le i - j_1$, and $G(iT) - G((i - j_1)T + (\pi - \alpha_1)T) = j_1 \bar{g} T = j_1 \pi CT$. Thus $k_0 \ge (j_1 + 1)\frac{\pi TC}{L} = \frac{j_1+1}{j_1+\alpha_1}\pi \bar{K}$.

   (b) If $\pi > \alpha_1$, then $i - j_1 < i - j_1 + \pi - \alpha_1 \le i - j_1 + \pi$, and $G(iT) - G((i - j_1)T + (\pi - \alpha_1)T) = j_1 \pi CT - (\pi - \alpha_1)CT$. Thus $k_0 \ge (j_1 + \frac{\alpha_1}{\pi})\frac{\pi TC}{L} = \frac{j_1 + \frac{\alpha_1}{\pi}}{j_1+\alpha_1}\pi \bar{K}$.

   Thus the first equation is equivalent to $k_0 \ge k_1$. Similarly we can prove that the second equation is equivalent to $k_0 \le k_2$. Therefore the second scenario in (14) is proved.

2. When $G((i - j_1)T + (\pi - \alpha_1)T) + k_0 L < G(iT) + \pi TC$; i.e., if $k_0 < k_1 \le k_2$, then $\bar{g} < \pi C$, and from (13) we have

$$G(iT) + \bar{g}T \;=\; G((i - j_1)T + (\pi - \alpha_1)T) + k_0 L.$$

   When $\pi \le \alpha_1$, we have $\bar{g} = \frac{k_0 L}{(j_1+1)T} = \frac{k_0}{k_1}\pi C$. When $\pi > \alpha_1$, we have

$$(j_1 + 1)T\bar{g} - \int_0^{(\pi-\alpha_1)T} g(t)dt \;=\; k_0 L.$$

   If we assume that $g(t)$ is evenly distributed between 0 an πT, then $\int_0^{(\pi-\alpha_1)T} g(t)dt = (1 - \frac{\alpha_1}{\pi})T\bar{g}$, and $\bar{g} = \frac{k_0}{k_1}\pi C$. Therefore the first scenario in (14) is proved.

3. When $G((i - j_2)T + (\pi - \alpha_2)T) + (K - k_0)L < G(iT) + \pi TC$; i.e., if $k_0 > k_2$, then $\bar{g} < \pi C$, and from (13) we have

$$G(iT) + \bar{g}T \;=\; G((i - j_2)T + (\pi - \alpha_2)T) + (K - k_0)L.$$

When $\pi \leq \alpha_2$, we have $\bar{g} = \frac{(K-k_0)L}{(j_2+1)T} = \frac{K-k_0}{K-k_2}\pi C$. When $\pi > \alpha_2$, we have

$$(j_2+1)T\bar{g} - \int_0^{(\pi-\alpha_2)T} g(t)dt \;\; = \;\; (K-k_0)L.$$

If we assume that $g(t)$ evenly distributes from 0 to πT, then $\int_0^{(\pi-\alpha_2)T} g(t)dt = (1-\frac{\alpha_2}{\pi})T\bar{g}$, and $\bar{g} = \frac{K-k_0}{K-k_2}\pi C$. Therefore the third scenario in (14) is proved.

■

Acknowledgments

The first author would like to thank the support of a UCCONNECT faculty grant.

References

References

Ardekani, S., Herman, R., 1987. Urban network-wide traffic variables and their relations. Transportation Science 21 (1), 1--16.

Buisson, C., Ladier, C., 2009. Exploring the impact of homogeneity of traffic measurements on the existence of macroscopic fundamental diagrams. Transportation Research Record: Journal of the Transportation Research Board 2124, 127--136.

Cassidy, M., Jang, K., Daganzo, C. F., 2011. Macroscopic fundamental diagrams for freeway networks. Transportation Research Record: Journal of the Transportation Research Board 2260, 8--15.

Chang, T.-H., Lin, J.-T., 2000. Optimal signal timing for an oversaturated intersection. Transportation Research Part B: Methodological 34 (6), 471--491.

Chang, T.-H., Sun, G.-Y., 2004. Modeling and optimization of an oversaturated signalized network. Transportation Research Part B 38 (8), 687--707.

Daganzo, C. F., 1995. The cell transmission model II: Network traffic. Transportation Research Part B 29 (2), 79--93.

Daganzo, C. F., 2005a. A variational formulation of kinematic waves: basic theory and complex boundary conditions. Transportation Research Part B 39 (2), 187--196.

Daganzo, C. F., 2005b. A variational formulation of kinematic waves: Solution methods. Transportation Research Part B 39 (10), 934--950.

Daganzo, C. F., 2007. Urban gridlock: Macroscopic modeling and mitigation approaches. Transportation Research Part B 41 (1), 49--62.

Daganzo, C. F., Gayah, V. V., Gonzales, E. J., 2011. Macroscopic relations of urban traffic variables: Bifurcations, multivaluedness and instability. Transportation Research Part B 45 (1), 278--288.

Daganzo, C. F., Geroliminis, N., 2008. An analytical approximation for the macroscopic fundamental diagram of urban traffic. Transportation Research Part B 42 (9), 771--781.
D'ans, G., Gazis, D., 1976. Optimal control of oversaturated store-and-forward transportation networks. Transportation Science 10 (1), 1--19.
Dion, F., Rakha, H., Kang, Y., 2004. Comparison of delay estimates at under-saturated and over-saturated pre-timed signalized intersections. Transportation Research Part B 38 (2), 99--122.
Evans, L., 1998. Partial Differential Equations. American Mathematical Society.
Gartner, N. H., Little, J. D., Gabbay, H., 1975. Optimization of traffic signal settings by mixed-integer linear programming: Part i: The network coordination problem. Transportation Science 9 (4), 321--343.
Gartner, N. H., Wagner, P., 2004. Analysis of traffic flow characteristics on signalized arterials. Transportation Research Record: Journal of the Transportation Research Board 1883, 94--100.
Gazis, D., Potts, R., 1963. The over-saturated intersection. In: Procedings of the 2nd International Symposium on Traffic Theory. Organisation for Economic Co-operation and Development, pp. 221--237.
Gazis, D. C., 1964. Optimum control of a system of oversaturated intersections. Operations Research 12 (6), 815--831.
Geroliminis, N., Boyaci, B., 2012. The effect of variability of urban systems characteristics in the network capacity. Transportation Research Part B 46 (10), 1607--1623.
Geroliminis, N., Daganzo, C. F., 2008. Existence of urban-scale macroscopic fundamental diagrams: Some experimental findings. Transportation Research Part B 42 (9), 759--770.
Geroliminis, N., Haddad, J., Ramezani, M., 2013. Optimal perimeter control for two urban regions with macroscopic fundamental diagrams: A model predictive approach. Intelligent Transportation Systems, IEEE Transactions on 14 (1), 348--359.
Godfrey, J., 1969. The mechanism of a road network. Traffic Engineering and Control 8 (8), 323--327.
Haberman, R., 1977. Mathematical models. Prentice Hall, Englewood Cliffs, NJ.
Improta, G., Cantarella, G., 1984. Control system design for an individual signalized junction. Transportation Research Part B: Methodological 18 (2), 147--167.
Jin, W.-L., 2015. Continuous formulations and analytical properties of the link transmission model. Transportation Research Part B 74, 88--103.
Jin, W.-L., Gan, Q.-J., Gayah, V. V., 2013. A kinematic wave approach to traffic statics and dynamics in a double-ring network. Transportation Research Part B 57, 114--131.
Jin, W.-L., Yu, Y., 2015. Asymptotic solution and effective Hamiltonian of a Hamilton-Jacobi equation in the modeling of traffic flow on a homogeneous signalized road. Journal de Mathématiques Pures et Appliquées (JMPA)In press.
Lighthill, M. J., Whitham, G. B., 1955. On kinematic waves: II. A theory of traffic flow on long crowded roads. Proceedings of the Royal Society of London A 229 (1178), 317--345.
Mahmassani, H., Williams, J., Herman, R., 1987. Performance of urban traffic networks.

Proceedings of the Tenth International Symposium on Transportation and Traffic Theory.
Miller, A. J., 1963. Settings for fixed-cycle traffic signals. Operations Research 14 (4), 373--386.
Moskowitz, K., 1965. Discussion of 'freeway level of service as in uenced by volume and capacity characteristics' by D.R. Drew and C. J. Keese. Highway Research Record 99, 43--44.
Munjal, P. K., Hsu, Y. S., Lawrence, R. L., 1971. Analysis and validation of lane-drop effects of multilane freeways. Transportation Research 5 (4), 257--266.
Newell, G. F., 1989. Theory of highway traffic signals. Tech. rep.
Newell, G. F., 1993. A simplified theory of kinematic waves in highway traffic I: General theory. II: Queuing at freeway bottlenecks. III: Multi-destination flows. Transportation Research Part B 27 (4), 281--313.
Olszewski, P., Fan, H., Tan, Y., 1995. Area-wide traffic speed-flow model for the singapore cbd. Transportation Research Part A 29 (4), 273--281.
Papageorgiou, M., 1995. An integrated control approach for traffic corridors. Transportation Research Part C: Emerging Technologies 3 (1), 19--30.
Papageorgiou, M., Diakaki, C., Dinopoulou, V., Kotsialos, A., Wang, Y., 2005. Review of road traffic control strategies. Proceedings of the IEEE 91 (12), 2043--2067.
Park, B., Messer, C. J., Urbanik, T., 1999. Traffic signal optimization program for oversaturated conditions: genetic algorithm approach. Transportation Research Record: Journal of the Transportation Research Board 1683, 133--142.
Richards, P. I., 1956. Shock waves on the highway. Operations Research 4 (1), 42--51.
Roess, R., Prassas, E., McShane, W., 2010. Traffic engineering. Prentice Hall.
Yperman, I., 2007. The link transmission model for dynamic network loading. Ph.D. thesis.
Yperman, I., Logghe, S., Tampere, C., Immers, B., 2006. The Multi-Commodity Link Transmission Model for Dynamic Network Loading. Proceedings of the TRB Annual Meeting.